JOURNAL OF MATERIALS SCIENCE 23 (1988) 4383–4391

The reversible enthalpy change of the metallic glass $Fe_{40}Ni_{40}B_{20}$ – Experiments and simulation in the activation energy spectrum model

E. WOLDT
Institut für Werkstoffe, Technische Universität Braunschweig, Postfach 3329, D-3300 Braunschweig, Federal Republic of Germany

The activation energy spectrum model can be used quite successfully to explain various aspects of the kinetics of structural relaxation in metallic glasses. In order to describe the often observed reversible component in a more quantitative way in the framework of this model an expression for the temperature dependence of the reversible part of the activation energy spectrum is derived. Using this expression three experiments concerning the reversible enthalpy change during structural relaxation are simulated and the results are compared with the actual experimental traces.

1. Introduction

Due to the inherently metastable character of the amorphous structure of metallic glasses the atoms are on the whole in less stable configurations than in crystals. Thermal activation will induce rearrangements for groups or single atoms. The sharply defined activation energies for these movements in crystals are likely to be smeared out in the case of an amorphous structure into a spectrum of activation energies.

This is a consequence of the different resultant force different atoms experience since their respective neighbouring atoms are in (merely) statistically predictable positions. The so-called activation energy spectrum (AES) model utilizes this idea as a starting point in its attempt to model some of the basic aspects of structural relaxation in metallic glasses.

This model has been used quite successfully to explain such phenomena as the often observed log–time kinetics of structural relaxation, the crossover effect and the reversibility of some property changes on cycling the annealing temperature.

This paper intends to show how the until now unspecified temperature dependence of the reversible component of the activation energy spectrum can be derived from a few assumptions. A comparison with some of the experimental data on this subject is included as well.

2. The basic features of the activation energy spectrum model

In the activation energy spectrum model an isothermal property change ΔP during structural relaxation is described by

$$\Delta P = \int_0^\infty c(E)q(E, T) \times \{1 - \exp[-\nu\, t \exp(-E/kT)]\}\, dE \quad (1)$$

where E stands for the activation energy, T the absolute temperature, t the time and ν the Debye frequency. The function $q(E, T)$ represents the potential number of processes available for relaxation with activation energy E at the annealing temperature T. The coupling function $c(E)$ determines how much property change a single relaxation process at activation energy E will contribute to the total change. The characteristic annealing function θ

$$\theta(E, T, t) = 1 - \exp[-\nu\, t \exp(-E/kT)] \quad (2)$$

varies between 1 and 0 and gives the probability that a relaxation process with activation energy E has taken place after time t at temperature T. For the origin of this equation see Primak [1]. With increased time t this function appears to sweep along the energy axis and the higher the annealing temperature is the faster this happens [2].

For many purposes a step approximation of θ, situated at

$$E_0 = kT \ln(\nu\, t) \quad (3)$$

can be used with sufficient accuracy.

The potential number of processes available for relaxation $q(E, T)$ is given by the difference of the distribution present at the beginning of the current experiment $Q(E)$ and the time-independent so-called "equilibrium" distribution $q_s(E, T)$ for the actual annealing temperature

$$q(E, T) = Q(E) - q_s(E, T) \quad (4)$$

(Equilibrium here refers to an ideal glass structure, thermodynamically of course the glassy state can only be metastable.) The initial distribution $Q(E)$ can either be a quenched-in distribution, in other words the result of some preceding treatment where the temperature was not known or not constant), or the result of a previous isothermal anneal hence another equilibrium distribution $q_s(E, T')$ (though only up to a certain activation energy as determined by the duration

0022–2461/88 $03.00 + .12

and temperature of that preceding anneal, e.g. approximately given by E_0).

The assumption of a temperature dependent equilibrium distribution $q_s(E, T)$ already implies the occurrence of reversibility effects during temperature cycling. However a quantitative analysis of experimental data of the reversible component of structural relaxation in metallic glasses can only be carried out on the basis of a well defined temperature dependence of the equilibrium distribution.

Of course this is also necessary in order to simulate the enthalpy change during constant heating rate experiments. Details will be described later but for initial simulations a temperature dependence of $q_s(E, T)$ given by $(T_f - T)^{-1/3}$ was used following a suggestion by Leake *et al.* [3]. The temperature T_f here corresponds to a kind of fictive temperature. However comparing the simulated results with the experimental data the ratio of the peak heights of the simulated endothermic and exothermic peaks was much to small. Only moving T_f very close to the final temperature of the heating ramp improved the situation. This, however, had to be rejected as physically rather unrealistic and initiated a close study of the temperature dependence of the equilibrium distribution $q_s(E, T)$.

3. The temperature dependence of the equilibrium distribution $q_s(E, T)$

The basic situation for reversible structural relaxation in metallic glasses can be described in simple terms by an ensemble of two level systems (TLS). Each level of a system represents the energy of one of two configurations in which a single atom or group of atoms can be found (see, e.g. [2] or [4]). In this picture any amorphous structure is determined by a particular distribution of populated (and unpopulated) levels. By grouping together all systems with the same energy difference between the levels (here called the level gap Δ) a particular structure is equivalent to a population set. The partition of *one* TLS now describes how many sites with the same gap Δ are found in the higher or lower energy state. The population set will change under thermal activation if the actual structure does not correspond to the partitions required by the momentary temperature. For example in the case of the as-quenched structure the population set might in part correspond to a higher temperature, the temperature of the quench. Under subsequent annealing (and even at room temperature) the population of the TLSs will change and approach an equilibrium state where changes forth and back over the activation energy barrier cancel in their net effect. (This however is a very simplified picture. In reality the level systems are coupled and population changes in one system will affect the levels (or the energy barrier) in other systems [5] which reflects the metastable character of the amorphous structure and in the long-run leads to its crystallization.) A change in the population of the two levels in order to form an equilibrium with the requirements of the momentary temperature is connected to a change in enthalpy due to the gain or loss of potential energy. (For simplicity the connected change in entropy will not be considered here.)

This allows calculation of the energy content of the upper level in equilibrium for sites of a chosen activation energy E. In equilibrium the population of the two levels (n^1, n^2) does not change

$$dn_s^1/dt = dn_s^2/dt = 0 \tag{5}$$

For small deviations from equilibrium the rate of change is assumed to follow a first-order chemical rate equation

$$dn/dt = -\nu n \tag{6}$$

where ν, the attack frequency, is given by

$$\nu = \nu_0 \exp(-E/kT) \tag{7}$$

reflecting the thermal activation of the process. With Δ representing the energy difference of the two levels (see Fig. 1) the flow forth and back can then be written as

$$dn/dt(1 \rightarrow 2) = n^1 \nu_0 \exp(-E/kT) \tag{8}$$

$$dn/dt(2 \rightarrow 1) = n^2 \nu_0 \exp[-(E + \Delta)/kT] \tag{9}$$

In equilibrium $dn/dt(1 \rightarrow 2) = dn/dt(2 \rightarrow 1)$, $n^i = n_s^i$ holds and hence

$$n_s^1/n_s^2 = \exp(-\Delta/kT) \tag{10}$$

gives the Boltzmann partition for the two levels in equilibrium. If it is further assumed that the number of sites having two levels with an energy gap Δ is constant

$$C(\Delta) = n_s^1 + n_s^2 \tag{11}$$

this can be used to express the number of sites in configuration 1 under equilibrium conditions

$$n_s^1(\Delta, T) = C(\Delta) \exp(-\Delta/kT)/[1 + \exp(-\Delta/kT)] \tag{12}$$

For a chosen activation energy barrier E the level split Δ is not fixed but can in principle take any positive value. (In the case of a negative gap the situation is just the mirror image of the same configuration with a positive difference and thus is covered only considering positive values for Δ.) The "excess" energy content of the "upper" configuration (level 1) referred to level 2 at any activation energy E is given by the integral over all possible gaps Δ

$$\varepsilon(T) = \int_0^\infty n_s^1(\Delta, T)\Delta \, d\Delta = \int_0^\infty C(\Delta) \exp(-\Delta/kT)/[1 + \exp(-\Delta/kT)]\Delta \, d\Delta \tag{13}$$

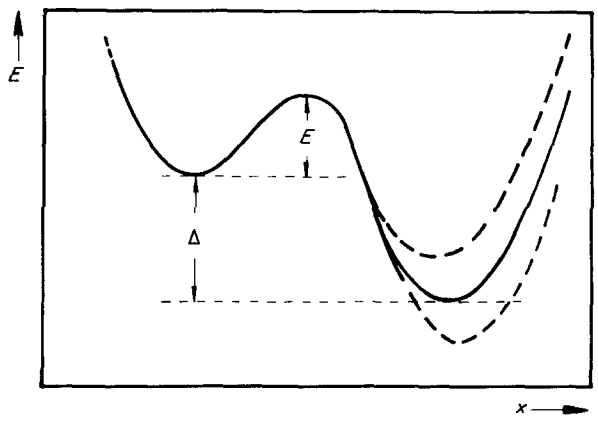

Figure 1 Energy levels for a schematic TLS.

If it is assumed, for simplicity only, that $C(\Delta)$ is a constant ($= C_\Delta$), the above integral can be evaluated substituting $\Delta/kT = x$

$$\varepsilon(T) = C_\Delta k^2 T^2 \int_0^\infty x/[\exp(x) + 1]\,dx$$
$$= C_\Delta k^2 T^2 \pi^2/12 \quad (14)$$

(for the integral see, e.g. [6]).

The last assumption implies that independently of the magnitude of the energy gap Δ there will be a constant number of sites with that gap. Obviously this is unrealistic for large values of Δ. A slightly more realistic approach is given by a constant distribution $C(\Delta)$ which falls off to zero at a certain value of Δ. As can be seen from Equation 14 this will only change the value of the numerical result of the integral but not the temperature dependence of $\varepsilon(T)$. In the even more realistic case where $C(\Delta)$ falls off to zero over a finite range the substitution of the integral will lead to a slightly modified temperature dependence of $\varepsilon(T)$. This, however, will not be very different from the T^2 dependence but since it is difficult to handle analytically if $C(\Delta)$ cannot be expressed as $C(x)$ it is excluded from the rest of the discussion.

Compared with the situation at absolute zero the structure contains additional enthalpy at any other temperature. The temperature dependence of this additional enthalpy can therefore generally be expressed by

$$\varepsilon(E, T) = A(E)T^2 \quad (15)$$

where $A(E)$ is constant for a fixed activation energy E. In the AES-model the additional enthalpy at a chosen activation energy E is given by the number of processes available for relaxation (with respect to absolute zero where no relaxation processes are possible) times the enthalpy that any of these processes releases during relaxation. In the formalism of the AES-model this can be written as

$$q_s(E, T)c_{\Delta H}(E) = \varepsilon(E, T) \quad (16)$$

This assumes implicitly that the equilibrium distribution $q_s(E, T)$ equals zero at $T = 0$. $c_{\Delta H}$ is the coupling function for the property change, in this case the enthalpy.

By combining both equations above, an expression for the temperature dependence of the equilibrium distribution $q_s(E, T)$ of the AES-model emerges

$$q_s(E, T) = A(E)/c_{\Delta H}(E)T^2 = n_0(E)T^2 \quad (17)$$

This means that the equilibrium distribution of processes available for relaxation is defined by the absolute temperature and a function $n_0(E)$ which depends only on the activation energy. The shape of the equilibrium distribution is given by $n_0(E)$ and the magnitude of the distribution at any activation energy E varies according to a T^2 dependence.

It should be noted that the derivation of Equation 14 is consistent with the recently developed, less approximate version of the AES model given by Hygate and Gibbs [7]. The treatment above also includes the term representing the transition from the lower energy state to the higher energy state. The interpretation of the meaning of $q_s(E, T)$ however differs from the new version of the model as pointed out by Hygate and Gibbs [7].

4. The coupling function for the enthalpy change in the AES model

According to the AES model any property change on structural relaxation is described by Equation 1 above. An isothermal anneal for time t_1 at high temperature T_1 will establish the equilibrium distribution of possible relaxation processes $q_s(E, T_1)$ as far as approximately $kT_1 \ln(\nu_0 t_1)$ along the activation energy axis. Any further isothermal anneals for temperatures smaller than T_1 and for times less than t_1 will cause property changes which correspond mainly to establishing the first part of a new equilibrium distribution. These changes, given the right experimental conditions, ought to be reversible.

If a second isothermal anneal at T_2 for a duration t_2 is assumed, the measured property change at any time during the second anneal can be described by

$$\Delta P(t) = \int_0^\infty c(E)$$
$$\times (q_s(E, T_1) - q_s(E, T_2))\theta(E, T_2, t)\,dE \quad (18)$$

If, for simplicity, the step function approximation for $\theta(E, T_2, t)$ is used the above equation becomes

$$\Delta P(t) = \int_0^{E_0} c(E)(q_s(E, T_1) - q_s(E, T_2))\,dE \quad (19)$$

with $E_0 = kT_2 \ln(\nu_0 t)$. Using the expression developed for $q_s(E, T)$ in the previous section this simplifies to

$$\Delta P(t) = (T_1^2 - T_2^2)\int_0^{E_0} c(E)n_0(E)\,dE \quad (20)$$

In the case of the enthalpy change as the property change a sensible hypothesis about the shape of the coupling function $c(E)$ can be made. As described in the previous section a certain activation energy (barrier) E will not be connected only with *one* TLS but will be found with a multitude of systems. Or, to put it the other way round, the level gap Δ to a first approximation will be independent of the barrier height in a system of isolated wells. This suggests that more or less the same distribution of Δ will be found with any chosen activation energy barrier E, be it small or large. Therefore a configuration change will produce *on average* the same change in potential energy independent of the activation energy necessary to induce this switch.

Under these assumptions the coupling function $c_{\Delta H}(E)$ for the enthalpy can be treated as a constant, $c_{\Delta H}$. Equation 20 simplifies to

$$\Delta H(t) = (T_1^2 - T_2^2)c_{\Delta H}\int_0^{E_0} n_0(E)dE \quad (21)$$

In this form the time dependence of the upper limit of the integral (see Equation 3) can be used to derive information about $n_0(E)$ from measured traces for $\Delta H(t)$ using the time derivative on both sides of the equation. A somewhat easier approach (considering the problems of determining the time derivative of experimentally measured functions with inevitable inaccuracies) is to choose a sensible distribution for

$n_0(E)$ and see how this fits the measured curve. This of course will not necessarily produce a unique solution. For the result of this procedure see below.

5. Measured and calculated enthalpy change during temperature cycling

Fig. 2 (symbols) shows the result of a DSC experiment measuring the reversible enthalpy change of $Fe_{40}Ni_{40}B_{20}$ by Sommer *et al.* [8]. Here the reversible heat flow $d\Delta H_{re}/dt$ was measured during isothermal periods at different annealing temperatures after steps of 20 K on a previously fully relaxed specimen [8]. The samples were cycled several times between two levels with a heating rate of $dT/dt = 320\,K\,min^{-1}$ and measured. Then the annealing temperature was increased by a further 20 K for a new cycle. Positive and negative heat flow was observed and integration gave the reversible relaxation enthalpy

$$\Delta H_{re} = \int_0^t |d\Delta H_{re}/dt|\, dt \qquad (22)$$

To account also for the short time interval during which the calorimeter had not reached equilibrium an extrapolation was used. The values so determined are plotted against the annealing temperature in Fig. 2 (symbols). Clearly a temperature dependence is noticeable. Equation 21 allows the effect of this kind of experiment in the AES model to be calculated. The temperature dependence in the equation is caused by the T^2 factor and the temperature dependence of the upper limit of the integral. Sommer *et al.* do not give the duration of their step anneals so a time of 180 sec was chosen to simulate their experiment. This should be sufficient since in an earlier paper [9] the same authors reckon that the reversible enthalpy reaction only takes about 100 sec.

There remains the choice of the shape of the distribution $n_0(E)$. For reasons that will be explained later a normalized Gaussian was used. By trial and error it was established that a centre value of $E_0 = 1.9$ eV and a width $\sigma = 0.18$ eV gave a good fit to the experimental data for $Fe_{40}Ni_{40}B_{20}$. The result is also shown in Fig. 2 (dashed line). Since the value of the coupling constant $c_\Delta H$ is not known the calculated curve was scaled using the experimental point for the highest temperature. It has to be emphasized that the chosen distribution may still not give the best fit possible.

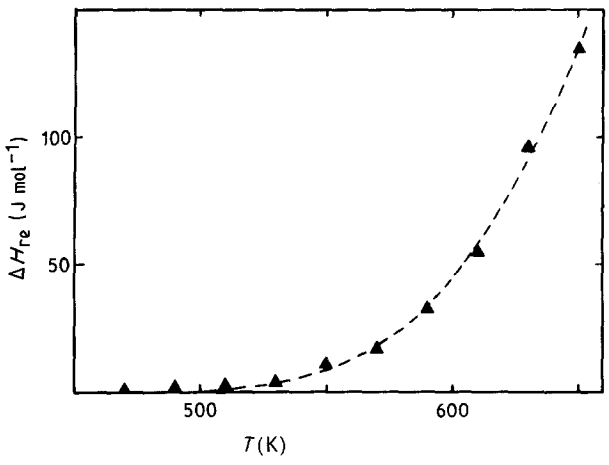

Figure 2 Data by Sommer *et al.* [8] for $Fe_{40}Ni_{40}B_{20}$ (▲) and calculated fit using a T^2 temperature dependence.

TABLE I Reversible enthalpy changes obtained from heat flow measurements after cooling and heating [10].

T_2 (K)	$\Delta H(600 \rightarrow T_2)$ (J mol^{-1})	$\Delta H(T_2 \rightarrow 600)$ (J mol^{-1})
590	−25	15
570	−40	40
550	−55	30
530	−35	15
510	−24	7

A further experiment investigating the reversible enthalpy change of $Fe_{40}Ni_{40}B_{20}$ was carried out by Görlitz *et al.* [10]. After an initial anneal to remove any irreversible relaxation effects (30 min at 620 K) the specimens were subjected to temperature steps between 600 K and a lower temperature T_2. While the temperature was held either at 600 K or T_2 for 15 min the heat flow dH_T/dt was recorded. The enthalpy change ΔH was then obtained by Görlitz *et al.* integrating over dH_T/dt with the lower limit equal to 30 sec (for experimental reasons) and the upper to 900 sec. Table I gives the results.

The values show that cooling is followed by an exothermic reaction and heating causes endothermic relaxation. This experiment can also be simulated in the AES model using Equation 21. Now, however, the lower limit of the integral also becomes temperature dependent. Care has to be taken especially in calculating the heating-up values. In this case the upper limit for the integral has to be $kT_2 \ln(\nu_0\ 900\,sec)$ even though the annealing function will move further along the energy axis at 600 K. However, the distribution beyond the above energy has not been altered by the low temperature anneal at T_2 and hence will not contribute to the endothermic reaction. Using the same distribution *and* scaling factor as for the data by Sommer *et al.* in Figure 2, the results of the simulation together with the values from Table I are presented in Fig. 3. The contours shown are calculated assuming different starting times for the integration of the heat flow after the temperature has reached its fixed level. The agreement is good considering the experimental error of 10% [11] especially since no further scaling was done.

To overcome the instrumental problems which distorted the heat flow at the beginning of the isothermal periods Görlitz *et al.* also used a modified measuring procedure. In this case the difference between two runs was taken; one of which was completing the full cycle, while the other one only undertook the changes during the temperature ramps and omitted the isothermal anneals. By assuming that the distortions due to the fast ramps were the same for both runs, the difference gave the integrated heat flow for the entire duration of the isothermal period.

In a further experiment using this modified procedure, Görlitz *et al.* [10] varied the length of the isothermal periods at 530 K before measuring the heat flow after reheating to 600 K. The result is shown in Fig. 4 (full line) together with the values calculated from the AES model with the lower integration limit

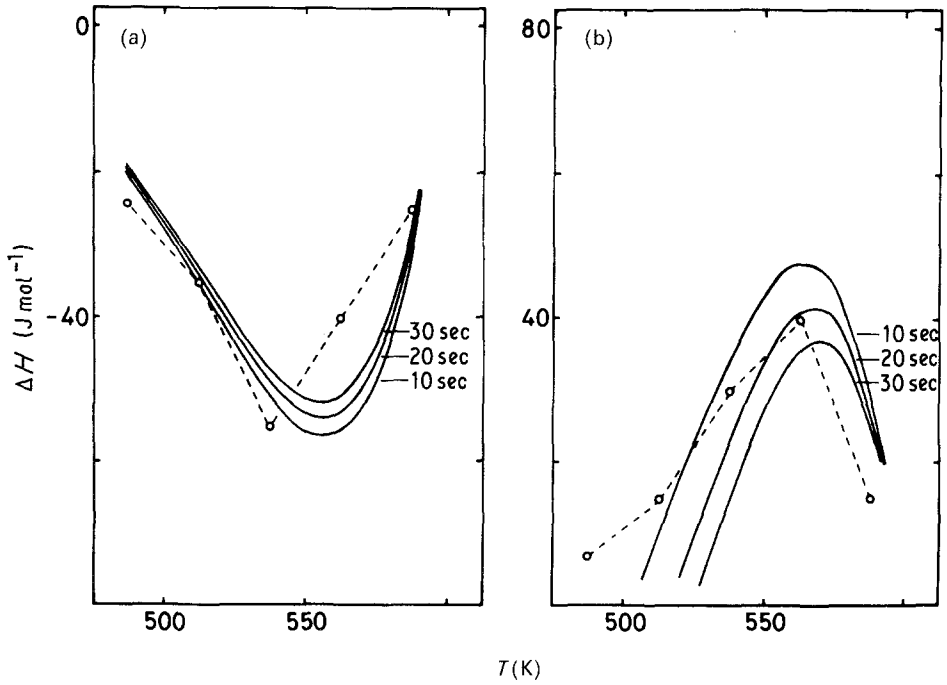

Figure 3 Reversible enthalpy changes in the experiment of Görlitz *et al.* [10] (○). The contours are calculated using the AES model for different lower integration limits. (a) ΔH (600 K → T_2) (b) ΔH (T_2 → 600 K).

assumed to be 0.1 sec. The agreement is good for short times; at later times the calculated curve (dashed) is still increasing while for the measured points the rise clearly slows down. On the activation energy scale the last point corresponds to 1.72 eV which is still on the rising flank of the Gaussian distribution chosen (centred at 1.9 eV). Therefore the deviation in Fig. 4 seems to indicate that in this range the Gaussian shape is no longer a good approximation of the true distribution.

6. Simulation of anisothermal measurements of apparent specific heat

6.1. Basis of the simulation

Fig. 5b shows the result of a DSC experiment to measure the enthalpy change of $Fe_{40}Ni_{40}B_{20}$ on linear heating (Majewska-Glabus *et al.* [12]). One as-quenched and a number of preannealed specimens have undergone a linear heating program ($dT/dt = 20\,K\,min^{-1}$) followed by rapid cooling back to room temperature and a second scan with $20\,K\,min^{-1}$. The difference between the first and second heating run is plotted against the annealing temperature in Fig. 5. The percentage values refer to the preannealing temperature as a fraction of the glass temperature T_g (which was assumed to be 685 K). The duration of the preanneals was always 15 min and the temperature scans extended to 20 K below the glass temperature.

This kind of experiment can also be simulated using the AES model. In this case, however, reversible and irreversible effects contribute to the result and the temperature is not constant. Therefore a simplified equation like Equation 21 cannot be used. If we retain the assumption that the coupling function $c(E)$ for the enthalpy change is a constant, $c_{\Delta H}$, and that the temperature dependence of the equilibrium distribution is given by T^2, Equation 23 describes the *isothermal* enthalpy change at temperature T of an arbitrary

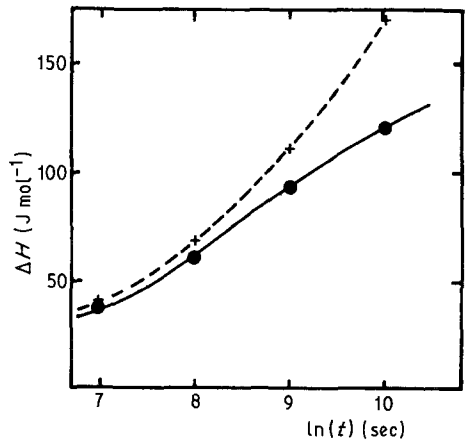

Figure 4 Reversible enthalpy change recorded at 600 K after preanneals of different duration at 530 K [10]. The dashed curve is calculated using the AES model.

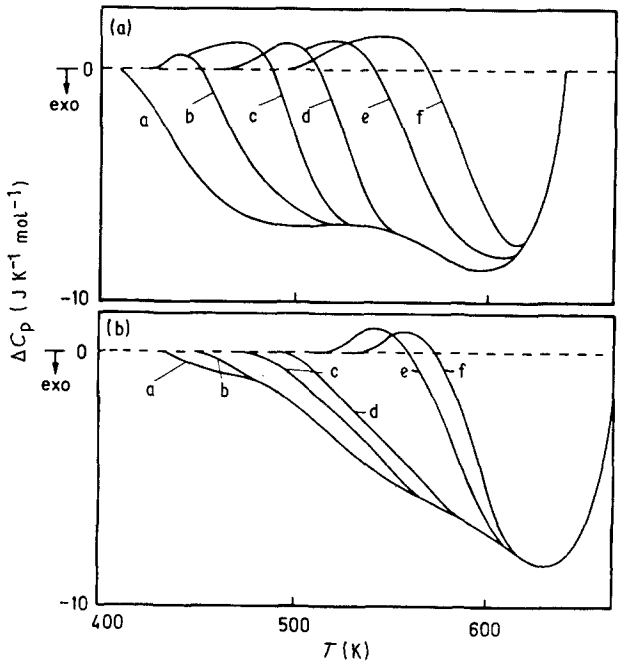

Figure 5 DSC curves for as quenched and preannealed specimens of $Fe_{40}Ni_{40}P_{20}$ (top) and $Fe_{40}Ni_{40}B_{20}$ (bottom) plotted with respect to the second scan, t_a = 15 min. (a) as quenched 52%, 56%, (b) 62%, (c) 67%, (d) 71%, (e) 75%, (f) 80% of T_g.

TABLE II Flow chart of the thermal history simulated for the "samples".

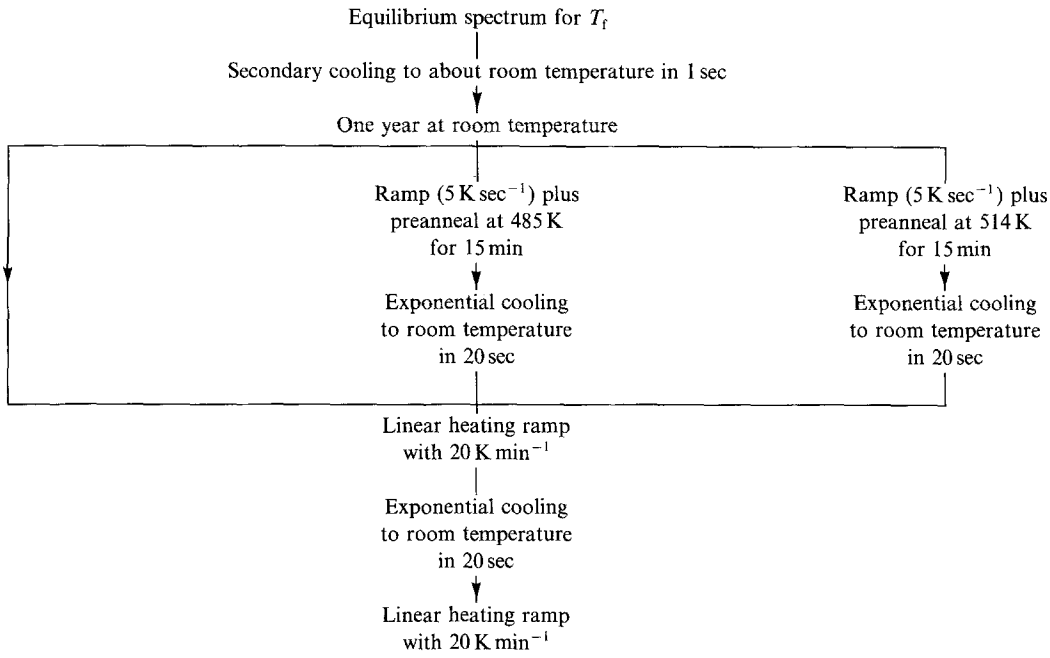

initial distribution of processes $Q(E)$

$$\Delta P(T, t) = c_{\Delta H} \int_0^\infty (Q(E) - n_0(E)T^2)\theta(E, T, t)\, dE \quad (23)$$

This equation allows a linear heating program to be treated as a succession of small isothermal steps whereby the final distribution at the end of one step is used as the initial distribution for the next step at slightly different temperature. At the new temperature a new equilibrium distribution is required and a small change in kinetics (θ function) will also take place. During the "isothermal" time of the step this will modify the distribution (and contribute to the property change) and produce a new final distribution which will become the initial distribution for the next step.

Along these lines a Fortran program was developed that approximates the linear heating ramp by 200 isothermal steps. For each step the change in the spectrum which ranges from 0 to 2.25 eV was calculated for 200 nodes based on the "isothermal" Equation 23. To obtain the property change per step the change in distribution at all nodes was then added up. Since all temperature steps are of the same duration the property change per step is equivalent to a rate of property change for the linear ramp. A further summation over this rate yields the total property change.

6.2. Initial conditions and simulated treatment

Two further questions had to be answered before the calculation could start: (1) What was to be chosen as starting distribution? and (2) What thermal history had to be considered for each specimen? The starting spectrum was assumed to represent the equilibrium distribution $q_s(E, T)$ of the temperature at the moment of the quench. This temperature can only be guessed and the limits are the glass temperature and the melting point. Under normal circumstances this equilibrium cannot be achieved again without crystallizing the specimen. This is equivalent to the concept of the fictive temperature (see, e.g. Egami [13]) and this temperature will, therefore, be called T_f from now on. In addition it was assumed that the material does undergo secondary cooling when it lifts off the melt spinning wheel during the production process. For the purpose of the program, this was treated as exponential cooling from the quench temperature (taken as T_f) to 10 K above room temperature in 1 sec plus linear cooling for 10 sec for the remaining 10 K temperature difference. Further it was assumed that the material had been stored at room temperature for one year before it was actually used in the DSC experiment.

This treatment was taken to define the distribution of possible relaxation processes present at the beginning of the real experiment for "as-quenched" material. The simulation usually looked at three "specimens". The first one was calculated to represent an "as-quenched" sample. This comprised a linear heating ramp followed by an exponential cooling back to about room temperature (in 20 sec) and a second heating ramp. In addition two "preannealed" specimens were calculated. Here the thermal history consisted of a quick ramp up to the annealing temperature ($dT/dt = 5$ K sec) and a 15 min anneal followed by an exponential cooling back to room temperature and then the same treatment as for the "as-quenched" specimen. Since the main interest was to see whether the endothermic effects observed in the real experiment could be reproduced, the preannealing temperatures were chosen as 71% and 75% of the glass temperature (compare with Fig. 5). The flow chart in Table II summarizes the thermal history of all "samples" during the different stages of the simulation.

6.3. Results and discussion of the simulation

Initially, mainly for simplicity, a box spectrum extending from 0 to 2.25 eV was chosen for $n_0(E)$, the shape

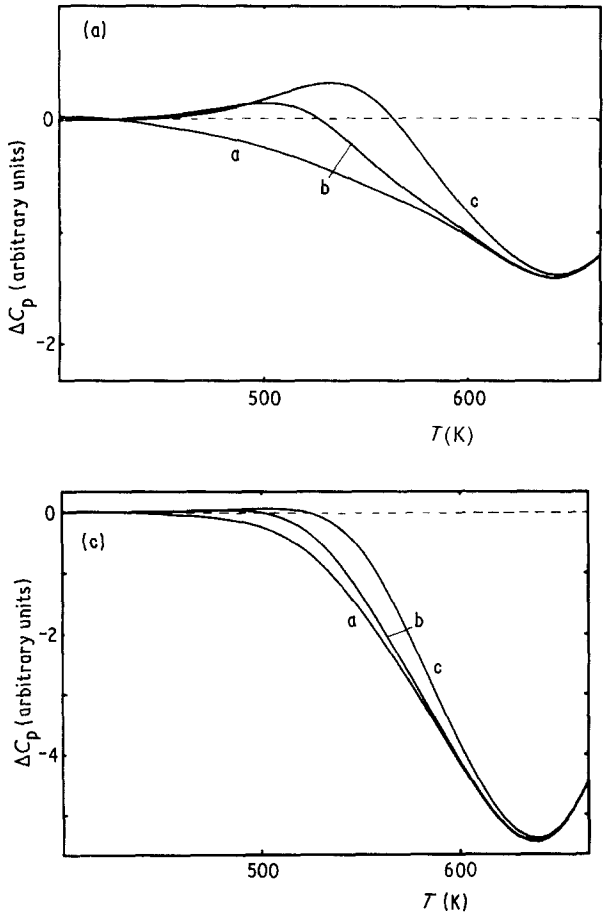

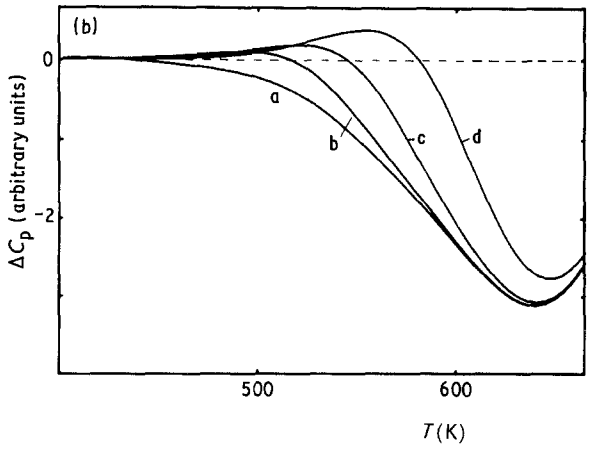

Figure 6 Simulation runs of the apparent specific heat of $Fe_{40}Ni_{40}B_{20}$ as in the experiment by Majewska-Glabus *et al.* [12] (Fig. 5) with initial fictive temperatures of (a) 710 K, (b) 800 K and (c) 1000 K. σ = 0.38, (a as quenched, b 71%, c 75%, d 80%).

of the equilibrium distribution $q_s(E, T)$. The fictive temperature was taken from the interval 700–1000 K and the temperature dependence of $q_s(E, T)$ was assumed to be $(T_f - T)^{-1/3}$ [3].

However, after a few simulation runs varying T_f it became clear that any distribution including activation energies significantly less than 1 eV would produce an endothermic peak on the as-quenched curve of similar magnitude as for the preannealed samples. This peak is due to the low energy processes relaxing during the secondary cooling and the subsequent one year at room temperature. These processes are reinstated during the first part of the heating ramp because of the shift of the equilibrium distribution to higher values. Experimental evidence (see, e.g. [8]) suggested a bell shaped spectrum of much smaller extent. Therefore, Gaussian shaped distributions falling off to very small values below 1 eV were used for further simulations. These did reduce the height of the peak on the as-quenched curve drastically. However the ratio of peak heights between endothermic and exothermic peaks was still too small compared with the real data (Fig. 5). As mentioned before only moving T_f very close to the upper temperature of the heating ramp improved this situation. This was rejected as physically rather unrealistic.

A small theoretical study as outlined above showed that a T^2-dependence for the equilibrium distribution might be close to the real situation. Further simulation runs were calculated under this assumption. By choosing T_f and so defining how much irreversible (in the sense of non-reinstateable) contribution was present in the initial "material" the peak ratio could be adjusted to resemble the experimental data. Based on the measurement of the self-diffusion energy of iron in $Fe_{40}Ni_{40}B_{20}$ by Horvath *et al.* [4] which gave a value of 2.4 eV, the Gaussians were centred at 2.4 eV as well. Fig. 6 shows the result of three complete simulations with the initial fictive temperatures of 710 K, 800 K and 1000 K using the above Gaussian with a width of σ = 0.38 eV.

All three runs show endothermic peaks (note the different scales) and the ratio of peak heights between endothermic and exothermic peaks depends strongly on the choice of T_f. While the overall features resemble the experimental traces quite well, there are differences in detail, so the endothermic peaks on the as-quenched and 71% curve. These become more pronounced for lower T_f values. For T_f = 800 K the peak ratio for the 75% curve is well matched with the experimental ratio, the way the traces join up before the minimum however differs. Also the additional calculated curve for the preanneal at 80% of the glass temperature still increases in endothermic peak height unlike the corresponding experimental trace. Fig. 7a demonstrates what happens if the width of the Gaussian (σ = 0.51 eV) is increased (T_f = 710 K). The centre part of the as-quenched curve as well as the way the curves join up around the minimum become more similar to the experiment. Again the endothermic peaks for the as-quenched and the 71% curves disagree with the experiment as does the ratio of the peak heights.

An increase of T_f to 800 K improves the result as shown in Fig. 7b. Now the peak ratio for the 75% curve is correct and the endothermic peaks for 75% and 80% appear at the correct temperature. Though the centre part of all the curves resembles the experimental traces quite well, the endothermic peaks for the as-quenched curve and the 71% preanneal cannot be found in the result for $Fe_{40}Ni_{40}B_{20}$. Also the increased peak height for the 80% curve, as well as the way it joins after the minimum, are different from the measured traces.

All these differences are a consequence of the uncertainty about the true shape of the equilibrium distribution. This can be seen in comparison with results for other materials. Majewska-Glabus *et al.* [12] also give

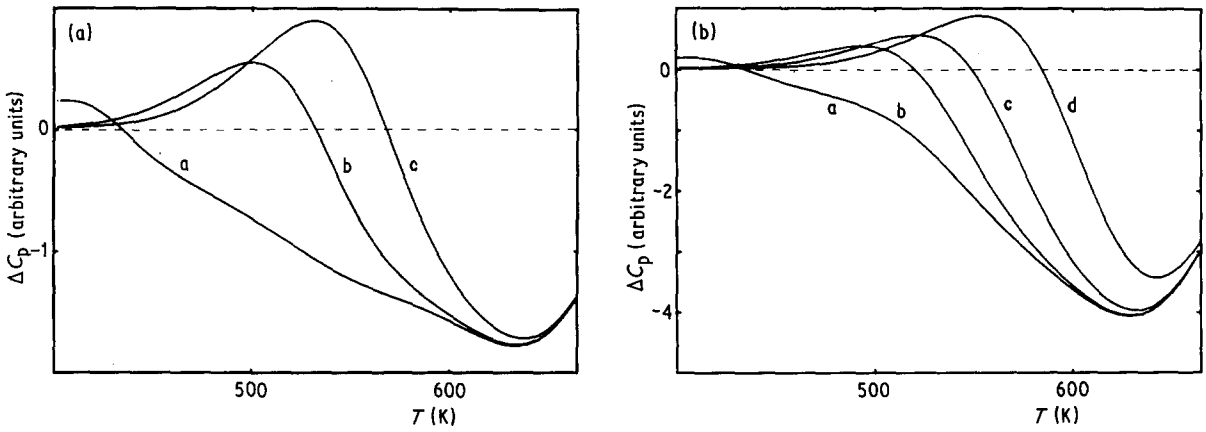

Figure 7 (a) As Fig. 6 but with increased width of the distribution, T_f = 710 K, (b) as above but with T_f = 800 K. σ = 0.51.

the traces for $Fe_{40}Ni_{40}P_{20}$ (see Fig. 5). Here the endothermic peaks already appear at much lower preannealing temperatures similar to the results in Fig. 7b. Inoue *et al.* [15] have found measuring, for example, $(Fe_{0.5}Ni_{0.5})_{75}Si_{10}B_{15}$ traces for the apparent specific heat that join at high temperatures in a similar fashion to Fig. 7b (see Fig. 8).

Another effect observed by Drijver *et al.* [16] is also very well reproduced by the simulation in the AES model. Fig. 9 shows the measured change for an endothermic peak after longer preanneals. A qualitatively similar result comes out of the simulation in the AES model (see Fig. 10).

7. Summary of the enthalpy change simulations

In summary this paper shows that the use of T^2 as temperature dependence of q_s (E, T) and a sensible choice of T_f do allow simulation of the main features of linear heating and isochronal experiments. For $Fe_{40}Ni_{40}B_{20}$ the use of a Gaussian shape for the spectrum of activation energies gives good agreement with the experimental data of Majewska-Glabus *et al.* [12], Sommer *et al.* [8] and Görlitz *et al.* [10]. However the fact that two distinct Gaussians, though not very different in the important range, appear to give the best fit to the isochronal experiments and the linear heating experiment, respectively, underlines that the true shape of the spectrum is still rather uncertain. This is also emphasized by the deviation between the calculated behaviour and the experiment at high temperatures [12] or long times [10]. Both cases seem to indicate that the spectrum in fact levels out instead of rising further. The uncertainty about the true shape of the initial part of the spectrum however is only of the same order as the variation in relaxation behaviour of different alloy compositions.

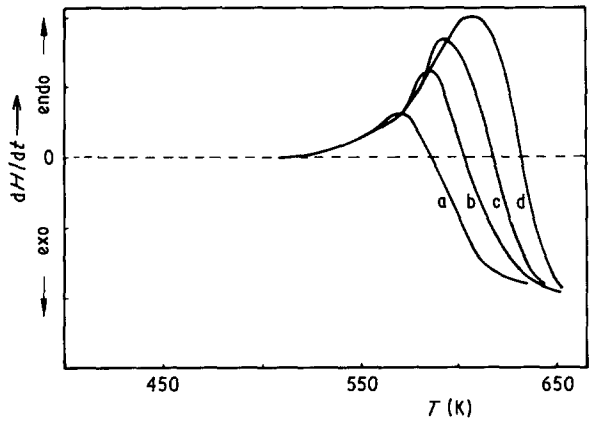

Figure 9 DSC scans of $Fe_{40}Ni_{40}B_{20}$ after preanneals of different duration (a 1 h, b 4 h, c 16 h, d 64 h) plotted with respect to the second scan [16].

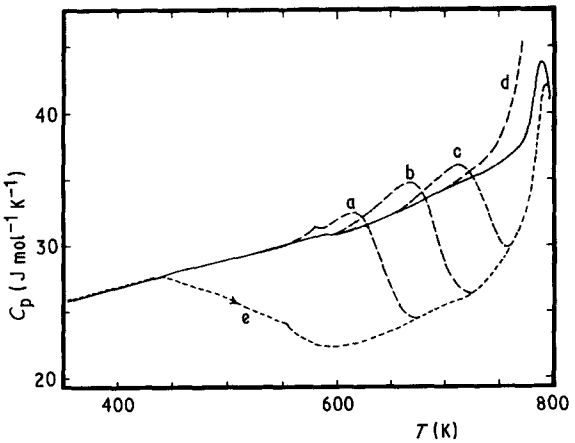

Figure 8 Specific heat of amorphous $(Fe_{0.5}Ni_{0.5})_{75}Si_{10}B_{15}$ for preanneals at different temperatures. Note here c_p not Δc_p is plotted [15]. t_a = 3 h (a 550 K, b 600 K, c 650 K, d 700 K, e as quenched).

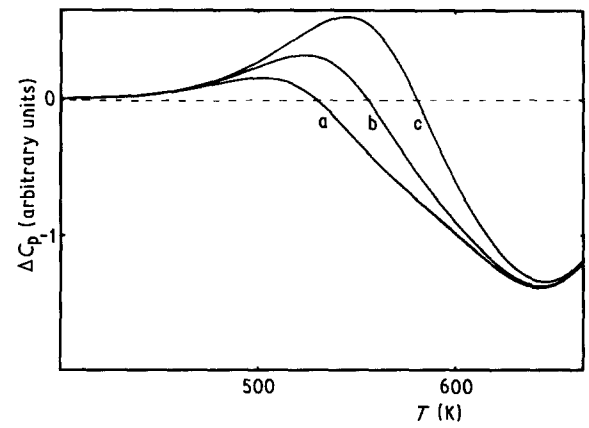

Figure 10 Simulation of the effect of preanneals of different duration T_a = 520 K (a 15 min, b 1 h, c 4 h) on the measurement of the specific heat in the AES model. T_f = 710 K, σ = 0.38.

Acknowledgements

The work described is part of a PhD thesis completed at the Department of Materials Science and Metallurgy, University of Cambridge, UK. I would like to thank everyone who got involved with the work in one way or the other, in particular Dr J. A. Leake and Dr J. E. Evetts for the encouragment and the initial stimulus and St John's College, Cambridge, for the studentship that made it all possible. I am also grateful to the SERC for the provision of equipment and to Professor Hull for laboratory facilities.

References

1. W. PRIMAK, *Phys. Rev.* **100** (1955) 1677.
2. M. R. J. GIBBS, J. E. EVETTS and J. A. LEAKE, *J. Mater. Sci.* **18** (1983) 278.
3. J. A. LEAKE, M. R. J. GIBBS, S. VRYENHOEF and J. E. EVETTS, in *J. Non-Cryst. Solids* **61&62** (1984) 787.
4. H. KRONMÜLLER, *Phil. Mag.* **48** (1983) 127.
5. J. E. EVETTS, in Proceedings of the 5th International Conference on Rapidly Quenched Metals, Würzburg, FRG September 1984, edited by S. Steeb and H. Warlimont (North Holland Physics Publishing, Amsterdam, 1985) p. 607.
6. I. N. BRONSTEIN and K. A. SEMENDJAJEW, in 'Taschenbuch der Mathematik", (Verlag Harry Deutsch, Frankfurt, 1980) p. 118.
7. G. HYGATE and M. R. J. GIBBS, *J. Phys. F* **17** (1987) 815.
8. F. SOMMER, H. HAAS and B. PREDEL, in Proceedings of the 5th International Conference on Rapidly Quenched Metals, Würzburg, FRG, September 1984, edited by S. Steeb and H. Warlimont (North Holland Physics Publishing, Amsterdam, 1985) p. 627.
9. F. SOMMER, H. HAAS and B. PREDEL, *J. Non-Cryst. Solids* **61&62** (1984) 793.
10. CH. GÖRLITZ and H. RUPPERSBERG, in Proceedings of the 5th International Conference on Rapidly Quenched Metals, Würzburg, FRG, September 1984, edited by S. Steeb and H. Warlimont (North Holland Physics Publishing, Amsterdam, 1985) p. 631.
11. CH. GÖRLITZ, Private communication.
12. I. MAJEWSKA-GLABUS and B. J. THIBJSSE, in Proceedings of the 5th International Conference on Rapidly Quenched Metals, Würzburg, FRG, September 1984, edited by S. Steeb and H. Warlimont (North Holland Physics Publishing, Amsterdam, 1985) p. 635.
13. T. EGAMI, in Proceedings of the 5th International Conference on Rapidly Quenched Metals, Würzburg, FRG, September 1984, edited by S. Steeb and H. Warlimont (North Holland Physics Publishing, Amsterdam, 1985) p. 611.
14. J. HORVATH, K. FREITAG and H. MEHRER, in Proceedings of the 5th International Conference on Rapidly Quenched Metals, Würzburg, FRG, September 1984, edited by S. Steeb and H. Warlimont (North Holland Physics Publishing, Amsterdam, 1985) p. 751.
15. A. INOUE, T. MASUMOTO and H. S. CHEN, *J. Mater. Sci.* **19** (1984) 3953.
16. J. W. DRIJVER, A. L. MULDER and S. RADELAAR, in Proceedings of the 4th International Conference on Rapidly Quenched Metals, Sendai, Japan, August 1981, edited by T. Masumoto and K. Suzuki, (The Japan Institute of Metals, Aoba Aramki, Sendai 980, Japan, 1982) p. 535.

Received 16 November 1987
and accepted 3 March 1988